Molecular Crystals and Liquid Crystals
Publication details, including instructions for authors and subscription information:
http://www.tandfonline.com/loi/gmcl20

Confined Colloidal Blue Phases with Potential for Photonics

Slobodan ŽUMER [a b c], Jun-Ichi Fukuda [a c d] & Miha Ravnik [a e]

[a] Faculty of Mathematics and Physics, University of Ljubljana, Slovenia

[b] Jozef Stefan Institute, Slovenia

[c] Center of Excellence NAMASTE, Slovenia

[d] National Institute of Advanced Industrial Science and Technology, Tsukuba, Japan

[e] Rudolf Peierls Centre for Theoretical Physics, University of Oxford, UK

Version of record first published: 13 Jun 2012.

To cite this article: Slobodan ŽUMER , Jun-Ichi Fukuda & Miha Ravnik (2012): Confined Colloidal Blue Phases with Potential for Photonics, Molecular Crystals and Liquid Crystals, 561:1, 107-114

To link to this article: http://dx.doi.org/10.1080/15421406.2012.687143

Mol. Cryst. Liq. Cryst., Vol. 561: pp. 107–114, 2012

ISSN: 1542-1406 print/1563-5287 online
DOI: 10.1080/15421406.2012.687143

Taylor & Francis
Taylor & Francis Group

Confined Colloidal Blue Phases with Potential for Photonics

SLOBODAN ŽUMER,[1,2,3,*] JUN-ICHI FUKUDA,[1,3,4] AND MIHA RAVNIK[1,5]

[1]Faculty of Mathematics and Physics, University of Ljubljana, Slovenia
[2]Jozef Stefan Institute, Slovenia
[3]Center of Excellence NAMASTE, Slovenia
[4]National Institute of Advanced Industrial Science and Technology, Tsukuba, Japan
[5]Rudolf Peierls Centre for Theoretical Physics, University of Oxford, UK

We have recently demonstrated various quasi-2D disclination networks in blue phases confined to thin layers, ranging from rings, skyrmions, to double helices, which can provide arrays of trapping sites for an easy assembling of colloidal particles in complex 2D lattice structures. In this brief review, we summarize main findings of our phenomenological modeling combined with topology. Effects of confinement, particle sizes and anchoring are discussed. Quasi-2D colloidal crystals can be easily manipulated by external stimuli via affecting liquid crystal or colloidal particles and offer means for novel applications in photonics.

Keywords Colloid; confined; blue phases; cholesteric liquid crystal; photonic crystal; self-assembly

1. Introduction

Self-assembled photonic crystals are of great interest for photonic and plasmonic applications [1]. By designing and optimizing the elementary building blocks—the colloidal particles—one can imprint into the material the needed inter-particle interactions, which lead to the assembly of the desired optical structures. The main challenge with the self-assembly approach is to produce regular structures with minimal number of structural defects.

A rather recent idea is to self-assemble optical structures by using colloids based on liquid crystalline solvents, which generate strong inter-particle potentials of multiple symmetries. Numerous structures can be assembled in nematic liquid crystals already with simple spherical particles where interactions are mediated either by localized nematic defects [2–4] or by nematic braids where entangling of particles by disclinations stabilizes the structures [5,6]. A special situation occurs when defects are used as traps for small colloidal particles [7]. Defects can be stabilized either by the confining geometry [8] or by

*Address correspondence to Slobodan Žumer, Faculty of Mathematics and Physics, University of Ljubljana, Slovenia. Tel.: +38614766500, Fax: +38612517281. E-mail: slobodan.zumer@fmf.uni-lj.si

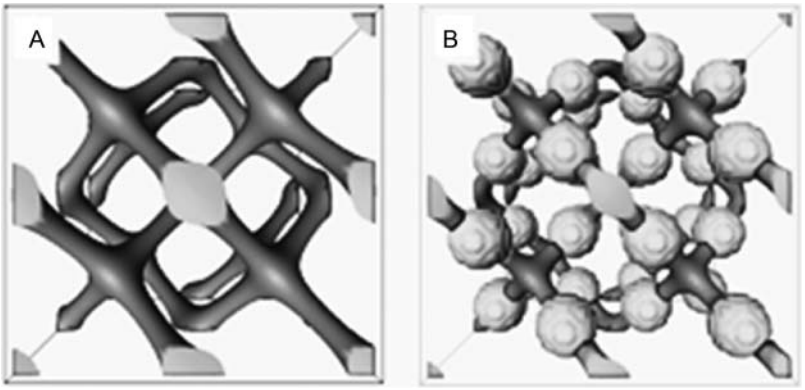

Figure 1. (A) Disclinations in BP II visualized as iso-surfaces of degree of order $S = 0.17$. (B) The same structure decorated by four colloidal particles per unit cell with 70 nm radius. $2 \times 2 \times 2$ unit cells with a 360 nm cubic cell are shown.

the complex chiral ordering like in blue phases [9]. In such phases strongly chiral nematic fluid exhibits periodic 3D modulation of the average molecular orientation [9]. These structures have a cubic network of orthogonal double-twist cylinders intercalated by $-1/2$ disclination lines [9]. These phases with a regular internal structure of the orientational order are the blue phase I (BP I) with a body centered cubic unit cell and the blue phase II (BP II) with a simple cubic cell (see Fig. 1(A)). Electrically controlled lasing was demonstrated in blue phase II by using the the periodicity of the blue phase lattice [10]. The use of the polymer stabilized BPs [11] was demonstrated for display applications [12,13]. Until recently very limited ($\sim$1 K) temperature stability region hindered further applications. However, recent developments that introduce blue phases with an extended stability range [14–16] regenerated a wide and new intrest in these advanced optical materials. These advances stimulated us to explore by numerical modelling and simulations the use of blue phases as templates for the self-assembliy of 3D colloidal crystals. The result for 3D BP II colloidal crystals is illustrated in Fig. 1(B) [17,18]. Blue phases confined to thin layers offer further possibilities for quasi 2D lattice structures ranging from helical disclinations to rings and skyrmions [19–21], that strongly depend on confinement. In this paper we briefly review our recent efforts to understand the organization of colloidal particles in such confined BP structures. Notably, because of their layered origin, these confined BP colloidal structures could be accessible in experiments by using the standard optical tweezers manipulation techniques. For more details see Ref. [22].

2. Blue Phases Confined to Thin Layers

The distinct profiles of orientational order in blue phases form as a result of the frustration appearing when chiral molecules helically order in more than one spatial direction. Effectively, this orienatational frustration gives rise to complex director profiles in the form of double twist cylinders which are intercalated by a regular network of defect lines with $-1/2$ winding number [9]. A delicate balance between the energetically favored regions of local double twist order and the energetic cost of disclination lines leads to two distinct

thermodynamically stable blue phases. BP I and BP II exhibit a three-dimensional crystalline orientational order corresponding to the cubic space groups O^{8-} and O^2, respectively. The lattice constants of blue phases are conditioned by the helicity (pitch) of the chiral nematic material and appear typically in the range of several hundred nanometers. We use phenomenological modeling to explore BPs based on the minimization of the Landau-de Gennes free energy [9]. The Landau-de Gennes free energy is a phenomenological expansion in terms of the symmetry-allowed invariants of the tensorial order parameter field $Q_{ij}(r)$ and its first derivatives. The traceless tensor incorporate all needed orientational degrees of freedom (director, degree of order S, and biaxiality). For details on the modeling approach see Refs. [9,18, and 19]. Our aim is the basic understanding of the phases, elasticity, and chirality; therefore only minimal number of invariants and associate material constants needed to construct the free energy are used. However, when relevant or needed in more quantitative study, the model can be directly and easily expanded to include also, e.g. the effects of different elastic constants and flexoelectricity. Elastic constant $L = 2.5 \times 10^{-11}$ N, phase constant $A_0 = 1.02 \times 10^5$ J/m^3 and reduced temperature parameter $\gamma = 3.375$ (A_0 and γ qualitatively map the standard A, B, C material constants in the Landau-de Gennes free energy, e.g see Ref. [18]), and the chiral parameter $q_0 = 2\pi/p_0$ corresponding to the intrinsic cholesteric pitch $p_0 = 0.556$ μm yield a BP II phase with 360 nm unit cell. The confinement to a thin layer is imposed by two flat surfaces that enforce homeotropic (perpendicular) surface anchoring of the liquid crystal, which is modeled as a quadratic penalty potential for any deviation of Q_{ij} from the surface preferred value. The strength of the potential characterized by the surface anchoring strength W_c ranges from 10^{-2} J/m^2 (strong) to 10^{-4} J/m^2 (effectively weak). The equilibrium BP order parameter profiles are obtained by minimizing the total free energy using the Euler-Lagrange formalism. The formalism gives a set of six coupled partial differential equations, one for each independent component of Q_{ij}, with an additional coupling condition Tr $Q_{ij} = 0$, which accounts for the $\mathbf{n} \rightarrow -\mathbf{n}$ symmetry of the nematic director. To solve the set of equations, the explicit Euler relaxation algorithm is used on a cubic mesh with the appropriate homeotropic boundary conditions at the top and bottom surfaces characterized by the anchoring strength W_c. In the lateral x and y directions, we assume periodic boundary conditions. The simulation box size is chosen to coincide with the size of one confined blue phase unit cell. The structures of confined blue phases are initialized as explained in Ref. [19], where the relaxation starts with a bulk blue phase I and is next confined by the top and bottom surfaces. The equilibrium cell size is calculated via the minimum in free energy at constant volumes. Note that this requires appropriate rescaling of the order parameter profiles.

To examine the stability of colloidal assemblies in confined blue phases, we select two topologically distinct and energetically most favorable confined blue phase structures: the *undulating-disclinations structure* with bulk disclination lines extending in two orthogonal directions and the *double-helix structure* (see Fig. 2) with bulk disclinations winding around a single direction in the form of a double helix. The undulating-discliantions structure is stable in a relatively thicker cells with weaker surface anchoring (we used cell thickness 0.7 μm and $W_c = 10^{-4}$ J/m^2), whereas the double-helix structure is stable in thinner cells with stronger surface anchoring (we used cell thickness 0.5 μm and $W_c = 10^{-2}$ J/m^2). These structures are in more detail described in Ref.[19], where a slightly different set of free energy parameters was used. Notably, in a thin cell with homeotropic anchoring and for materials with weaker twisting power, i.e. longer cholesteric pitches, the stable structures that emerge are a uniform lying helix (finger-print texture) or an untwisted uniform nematic profile.

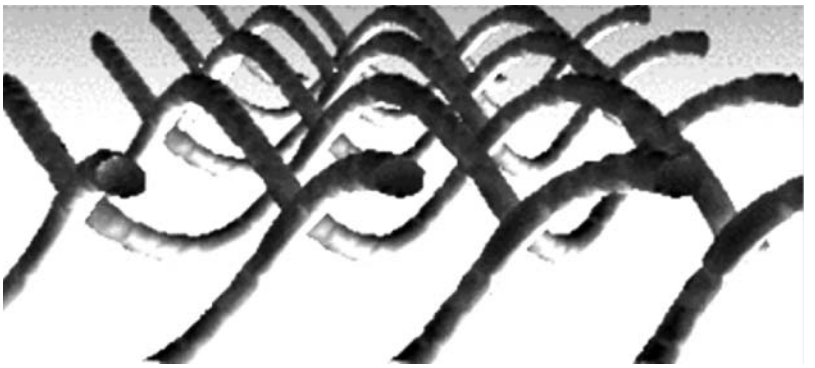

Figure 2. Confined blue phase structure: double-helix structure. Disclination lines are shown in gray as iso-surfaces of the degree of order $S = 0.25$ (bulk degree of order $\mathrm{Seq} = 0.41$).

Confinement and absence of a four-fold symmetry axis make the general unit cell of the confined blue phases a rectangle [19]. The equilibrium lattice constants are easily obtained from the free energy density profiles. Interestingly, the undulating disclinations structure close to the equilibrium behaves as almost an isotropic elastic medium, and its optimum shape is a square. On the other hand, the equilibrium unit cell size of the double-helix structure deviate significantly from the square, and its elastic response on e.g stretching in the lateral x and y directions is highly anisotropic.

3. Trapping Potentials in Thin Layers of Blue Phases

Nematic $-1/2$ disclination lines trap colloidal particles to reduce the effective volume of their highly distorted cores, e.g as we reported for $-1/2$ nematic disclination loops encircling large colloidal particles [8]. We have shown that this same concept can be applied also for trapping of colloidal particles by the disclination arrays in bulk cholesteric blue phases [17,18] and blue phased confined to thin layers [22]. In the regime of very weak particle surface anchoring, the trapping potential at a given location for a particle of distinct size can be calculated by integrating the free energy density of a particle-free confined blue phase over the same volume as would be occupied by the particle [22]. Similarly, also stabilization of blue phases by polymer matrices can be addressed [23]. The minima of the trapping potential (shown in dark gray in Fig. 3) for various particle sizes in both confined blue phase structures (undulating discliantions and double helices) show an increased localization of the trapping sites with an increasing size of the particles. At certain particle radius $\sim$100 nm also a change in the location of the minima from dislination lines to intermediate points is found. This means that particles small compared to the disclination core can be trapped anywhere in the disclination line region, whereas larger particles are more and more localized and trapped within trapping points, which can be even away from the disclinations. The change in the location of the minima to the intermediate points between two orthogonally-crossing lines happens when a single particle more optimally covers two neighboring lines rather than just a single one. It should be stressed that for particles with stronger anchoring, i.e. when nematic ordering around the particles is more distorted, the particle assembly cannot be directly modeled by simply observing such a potential. Figure 4 shows the profile of the trapping potential for a radius-100 nm particle in the undulating-disclinations blue phase structure via the iso-surfaces of different values

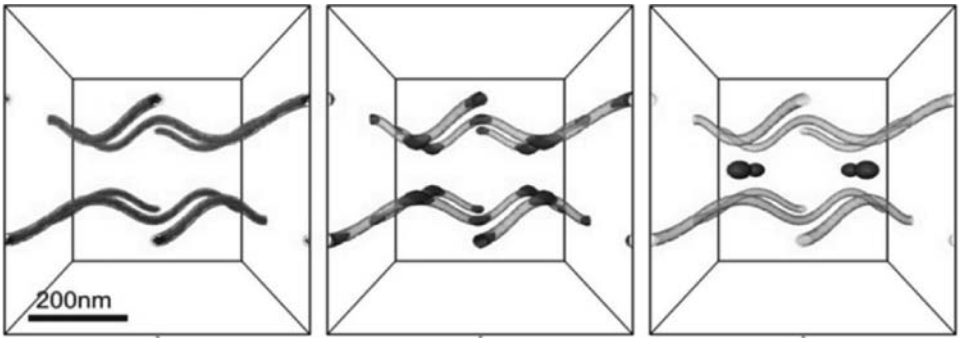

Figure 3. Minima of the trapping potential (in dark gray) for various particle sizes (left panel for radius of 40 nm, center panel for 80 nm, right panel for 120 nm) in the undulating-disclinations confined blue phase. Light gray shows the characteristic disclinations. 2 × 2 unit cells are drawn.

of the trapping potential. Interestingly, from the potential profile, one can extract also the energy barrier for a particle (with radius ∼100 nm) to cross from a trapping site at one disclination to the trapping site at another disclination to be in the range of 300 kT.

4. 2D and Quasi-2D Colloidal Crystals

Using the trapping potentials as determine above, the assembly of colloidal particles in the confined blue phases can be explored by filling the individual trapping sites with particles. Particles with radii from 40 nm to 140 nm and weak surface anchoring $Wp = 10^{-4}$ J/m^2 are used. We perform our calculations within one unit cell, however for clarity the structures are presented in 2×2 arrays of unit cells. Particles are initialized in the pre-predicted trapping sites and then their positions are equilibrated by shifting them to lower free energy positions after full equilibration of the liquid crystalline profile. Within the relaxation procedure the fluid flow is not considered expecting that the nematic profiles of the equilibrium configurations are not affected by the flow. However, the fluid flow may become of importance in the actual process of the structure formation—i.e. in

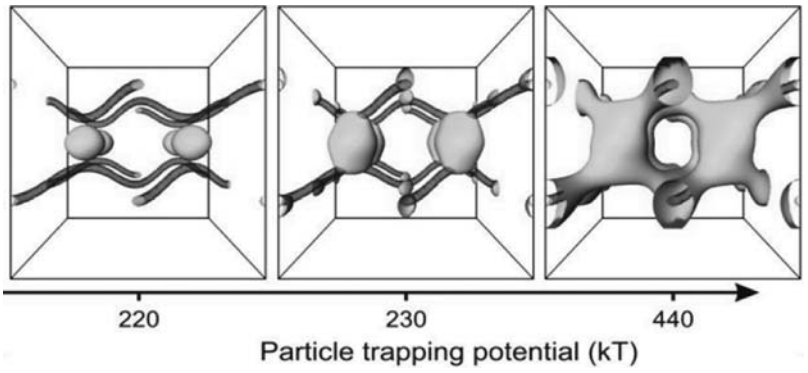

Figure 4. Iso-surfaces (in light gray) of various values of the trapping potential for a 100 nm particle in the undulating-disclinations confined blue phase. Dark gray shows the characteristic disclinations. 2 × 2 unit cells are drawn.

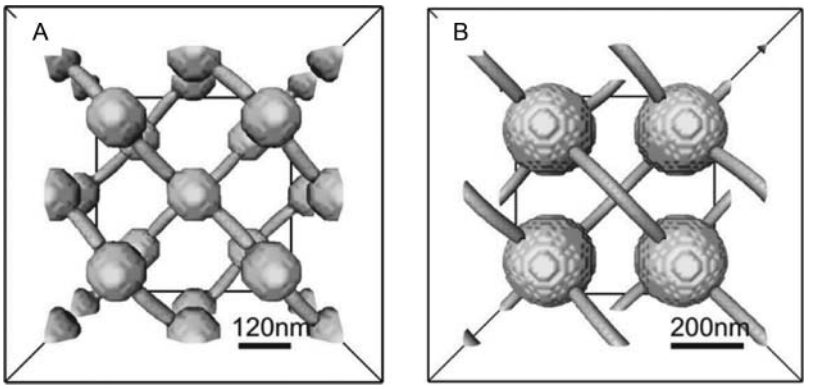

Figure 5. The optimal quasi-two-dimensional and two-dimensional colloidal crystals in the undulatating disclinations confined blue phase for particle radii 60 nm (A) and 120 nm (B). Dark gray shows the disclination regions. 2 × 2 colloidal unit cells are shown.

the dynamic trajectories how specific colloidal structures are assembled, by favoring or disfavoring specific restructuring possibilities leading to possible different (meta-) stable configuations.

Figure 5 shows quasi-2D and 2D colloidal crystals that assemble in the undulating disclination confined blue phase, depending on the size of the particles by filling the trapping sites shown in Fig. 3. For small particles (∼40 nm, Fig. 3 left panel), there are no distinct trapping sites in the undulating disclination structure and the particles can arrange arbitrarily within the disclinations as long as inter-particle interactions are weak. Therefore we focus on medium-sized (note Fig. 3 center panel) and large particles (Fig. 3 right panel). In the case of undulating-disclinations for particles with r = 60 nm, the energetically most preferred structure has 4 particles per unit cell (Fig. 5(A)). However, if the trapping sites are only partially filled, metastable colloidal structures are formed. Typically, they have their total free energies higher for ∼0.1%, corresponding to ∼100 kT, relative to the free energy of the stable energetically most preferred structure. Large particles ($r = 120$ nm) are trapped in the central mid-plane trapping sites linking two originally not connected disclinations and forming roughly a square lattice (Fig. 5(B)). The above results show that also more generally the trapping potential for particle sizes comparable to the cell thickness – the larger particles- (Fig. 5(B)) dictates two-dimensional ordering of particles. However, upon decreasing the size of the particles, they start to form layers yielding a quasi-two-dimensional regime of particle ordering (Fig. 5(A)). This regime also provides more freedom to form metastable structures with only partially filled trapping sites.

5. Conclusion

Two-dimensional and quasi-two-dimensional regular arrays of trapping sites are demonstrated for colloidal particles in blue phases confined to thin layers. The specific array of the trapping sites and its symmetry depend crucially on the size of the colloidal particles and on the size of the confined blue phase unit cell. Three trapping regimes are identified for particles with weak anchoring: (i) small particles get fully immersed in the strongly distorted disclination cores, (ii) medium-sized particles get trapped by the disclinations but they are affected also by the relative arrangements of the surrounfing double-twist cylinders

and therefore the trapping sites become points in a regular quasi 2D periodic array rather than lines, and (iii) large particles get not necessarily trapped within the disclinations, as they maximize the coverage of disclinations and minimize the coverage of the double-twist areas. Larger colloidal particles can also cause rewiring of disclinations. Depending on the filling of the available trapping sites, either stable or metastable colloidal structures form. Typically, for 100 nm particles with weak surface anchoring, the energy gain upon filling one trapping site is 0.1% of the total free energy of one confined blue phase unit cell.

Experimentally, by confining the blue phase liquid crystals to thin layers allows for the use of optical tweezers as an assembler tool. Such tweezers assisted assembly could avoid trapping of particles into metastable states, which is expected to be the main limitation in the self-assembly of regular colloidal structures in bulk blue phases. Notably, such study would need to optimize the typically leading tweezing mechanisms [24] to achieve strong enough effective coupling between the beam and the particles to be able to achieve efficient control over the particles: (i) the interaction of tweezers' laser beam with particles, which can be attractive or repulsive, depending on the relative refractive indices, (ii) the dielectric interaction of the laser beam with the LC distortion surrounding the colloidal particles, which is typically strongly anisotopic, and (iii) the effective elastic interaction due to laser-beam-induced distortion of the nematic order—both of the director and of the local degree of order. Speculatively, a possible tweezing approach would also be to melt into the isotropic phase locally the surrounding region of the particle using a high intensity beam, and then the particle could be shifted within such an "isotropic bubble". The (quasi) 2D structures also open more possibilities for possible manipulation of the structures with the external (electric or magnetic) fields via affecting the liquid crystal matrix and/or colloidal particles. The confined blue phases could offer potent templates for the self-assembled optical structures to be used in photonic and plasmonic applications.

Acknowledgements

The research was supported by the Slovenian Research Agency (P1-0099 & J1-2335), EU network HIERARCHY, and Center of Excellence NAMASTE. M. R. acknowledges support of the EC Marie Curie Program ACTOIDS. J.F. was in part supported by Grant-in-Aid for Young Scientists from Japan Society for Promotion of Science (JSPS).

References

[1] Wong, S., Kitaev, V., & Ozin, G. A. (2003). *J. Am. Chem. Soc.*, *125*, 15589.
[2] Poulin, P., Stark, H., Lubensky T.C., & Weitz, D.A. (1997). *Science*, *275*, 1770.
[3] Yada, M., Yamamoto, J., & Yokoyama, H. (2002). *Langmuir 18*, 7436.
[4] Muševič, I., Škarabot, M., Tkalec, U., Ravnik, M., & Žumer, S. (2006). *Science*, *313*, 954.
[5] Ravnik, M., Škarabot, M., Žumer, S., Tkalec, U., Poberaj, I., Babič, D., Osterman, N., & Muševič, I. (2007). *Phys. Rev. Lett.*, *99*, 247801.
[6] Tkalec, U., Ravnik, M., Čopar, S., Žumer, S., & Muševič, I. (2011). *Science*, *333*, 62.
[7] Pires, D., Fleury, J.-B., & Galerne, Y. (2007). *Phys. Rev. Lett.*, *98*, 247801.
[8] Škarabot, M., Ravnik, M., Žumer, S., Tkalec, U., Poberaj, I., Babič, D., & Muševič. (2008), *I. Phys. Rev., E 77*, 061706.
[9] Wright, D. C., & Mermin, N. D. (1989). *Rev. Mod. Phys.*, *61*, 385.
[10] Cao, W., Munoz, A., Palffy-Muhoray, P., & Taheri,(2002). *Nature Mater.*, *1*, 111–113.
[11] Kikuchi, H., Yokota, M., Hisakado, Y., Yang, H., & Kajiyama, T. (2002). *Nature Mater.*, *1*, 64.
[12] Hisakado, Y., Kikuchi, H., Nagamura, T., & Kajiyama, T. (2005). *Adv. Mater.*, *17*, 2311–2315.
[13] Ge, Z., Gauza, S., Jiao, M., Xianyu, H., & Wu, S-T. (2009). *Appl. Phys. Lett. 94*, 101104.

[14] Coles, H. J., & Pivnenko, M. N. (2005).*Nature*, *436*, 997.
[15] Alexander, G. P., & Yeomans, J. M. (2006). *Phys. Rev. E*, *74*, 061706.
[16] Castles, F., Morris, S. M., Terentjev, E. M., & Coles, H. J. (2010). *Phys. Rev. Lett.*, *104*, 157801.
[17] Žumer, S., Ravnik, M., Porenta, T., Alexander, G. P., J., & Yeomans, J. M. (2010). *Proc. SPIE*, *7775*, 77750H.
[18] Ravnik, M., Alexander, G. P. J., Yeomans, J. M., and Žumer, S. (2011). *PNAS*, *108*, 5188.
[19] Fukuda, J., & Žumer, S. (2010). *Phys. Rev. Lett.*, *104*, 017801.
[20] Fukuda, J., & Žumer, S. (2011). *Phys. Rev. Lett.*,*106*, 097801.
[21] Fukuda, J., & Žumer, S. (2011). *Nature Commun*. *2*, 246.
[22] Ravnik, M., Fukuda, J., Yeomans, J. M., & Žumer, S. (2011). *Soft Matter*, *7*, 10144.
[23] Fukuda, J. (2010). *Phys. Rev. E*, *82*, 061702.
[24] Škarabot, M., Ravnik, M., Babič, D., Osterman, N., Poberaj, I., Žumer, S., Muševič, I., Nych, A., Ognzsta, U., & Nazarenko, V. (2006). *Phys. Rev. E*, *73*, 021705.